Computing Permanents for Boson Sampling on Tianhe-2 Supercomputer

Junjie Wu,[1,2,*] Yong Liu,[1,2] Baida Zhang,[2] Xianmin Jin,[3,4,†]
Yang Wang,[1,2] Huiquan Wang,[1,2] and Xuejun Yang[1,2,‡]

[1]*State Key Laboratory of High Performance Computing, National University of Defense Technology, Changsha 410073, China*
[2]*College of Computer, National University of Defense Technology, Changsha 410073, China*
[3]*State Key Laboratory of Advanced Optical Communication Systems and Networks, Institute of Natural Sciences & Department of Physics and Astronomy, Shanghai Jiao Tong University, Shanghai 200240, China*
[4]*Synergetic Innovation Center of Quantum Information and Quantum Physics, University of Science and Technology of China, Hefei, Anhui 230026, China*

(Dated: June 17, 2016)

Boson sampling, a specific quantum computation problem, is widely regarded to be one of the most achievable fields in which quantum machine will outperform the most powerful classical computer in the near term, although up to now no upper-bound of how fast the classical computers can compute matrix permanents, core problem of Boson sampling, has been reported. Here we test the computing of the matrix permanent on Tianhe-2, a supercomputer retaining its position as the world's No. 1 system for six times since June 2013. We arrived at the time (about $77.41 \sim 112.44$ minutes) to compute the permanent of a 50×50 matrix in an acceptable precision. In addition, we have found that Ryser's algorithm will produce an unacceptable error with the increase of problem scale, compared to Balasubramanian-Bax/Franklin-Glynn's algorithm in the same complexity. The precision issue suggests carefully check in future research of Boson sampling, and comprehensive comparison between quantum computer and classical computer.

arXiv:1606.05836v1 [quant-ph] 19 Jun 2016

I. INTRODUCTION

Universal quantum computers promise to substantially outperform classical computers [1, 2], however, they have been experiencing challenges to build in practice, due to stringent requirement of high-fidelity quantum gate and scalability. For example, Shor's algorithm [3], solving integer factorization problem, is one of the most attractive quantum algorithms because of its potential to crack current mainstream RSA cryptosystem. An universal quantum computer requires 1025 qubits to factor a 1024-bit number ($\sim 10^{307}$) [4, 5], a key size thought to be crackable on classical computers [6]. However, the largest number factored using Shor's algorithm is 21 untill now [4, 7–10]. This motivates the research of specific quantum computation with quantum speedup and more favorable experimental conditions.

Boson sampling [11] is a specific quantum computation thought to be an outstanding candidate for beating the most powerful classical computer in the near term. It samples the distribution of Bosons coming from a complex interference network. Unlike universal quantum computation, quantum Boson sampling seems to be more straightforward, since it only requires identical Bosons, linear evolution and measurement. As for classical computers, the distribution can be obtained by computing permanents of matrices derived from the unitary transformation matrix of the network [12]. However, computing the permanent has been proved as a #P-hard task with classical computers. The best-known classical algorithm scales exponentially with the size of a matrix. These motivate a lot of advances in building larger quantum Boson sampling machine to outperform classical computers, including principle-of-proof experiments [13–16], simplified models easy to implement [17–19], implementation techniques [20–23], robustness of Boson sampling [24–28], validation of a large scale Boson sampling [29–31], varied models for other quantum states [32–34], etc.

However, what is the upper-bound of computing the permanent on classical computer? Solving Boson sampling problem with N Bosons on classical computers depends on computing permanents of $N \times N$ matrices. Therefore, the upper-bound is strongly related to the condition on which a quantum Boson sampling machine will surpass classical computers.

Here we present the test results of computing permanents on Tianhe-2 [35] (FIG. 1), the supercomputer which has retained its position as the world's No.1 in Top500 supercomputer lists since June 2013. The performance of Tianhe-2 is comparable with that of several millions of typical personal computers working simultaneously. We developed, optimized and tested parallel programs of two best-known algorithms, Ryser's algorithm and Balasubramanian-Bax/Franklin-Glynn's (BB/FG's) algorithm. In this paper, we report the speed performance of Ryser's algorithm and BB/FG's algorithm in real tests on Tianhe-2 supercomputer. We then show the predicted performance of computing the permanent of a 50×50 matrix on the full system of Tianhe-2 supercom-

*Electronic address: junjiewu@nudt.edu.cn
†Electronic address: xianmin.jin@sjtu.edu.cn
‡Electronic address: xjyang@nudt.edu.cn

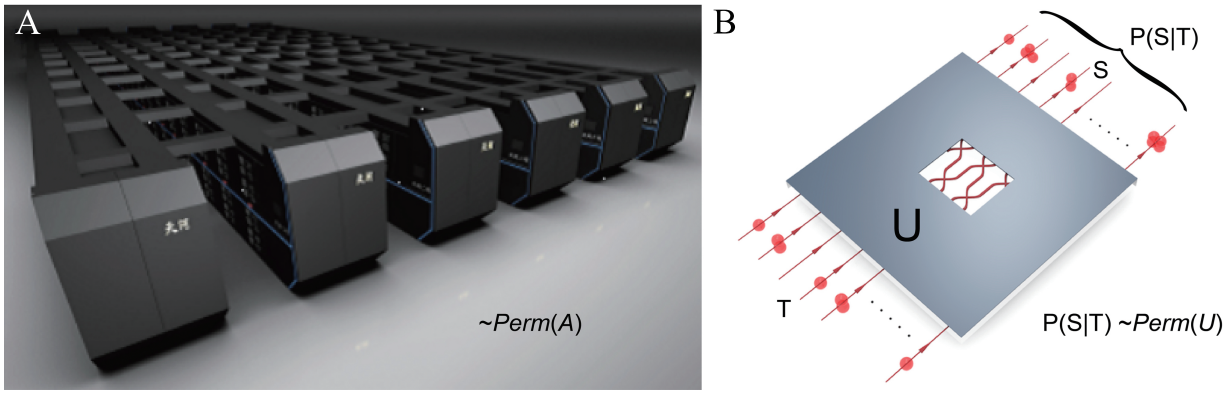

FIG. 1: **A schematic view of computational task on permanent with Tianhe-2 supercomputer (A) and quantum Boson sampling machine (B).** The computational power on calculating permanent of matrix A can be directly tested with different algorithms on Tianhe-2. The output probabilities P(S—T) can be obtained in quantum Boson sampling machine given a input state S, unitary operation matrix U and output state T, which is equivalent to compute the permanent of matrix U. The capacity of computing permanent on Tianhe-2 is employed to benchmark the state of arts and set an upper bound to be beaten by quantum Boson sampling machine.

puter. In addition, we show that Ryser's algorithm has an unacceptable accumulating rounding error from the limited word length of classical computers, compared to BB/FG's algorithm. This implies the result of Ryser's algorithm for large-size matrices may be untrustable.

II. RESULTS

Ryser's algorithm is shown in Equation (1) and BB/FG's algorithm in Equation (2). In the equations, $Perm(A)$ denotes the permanent of the matrix A. a_{ij} is the element of A in the ith row and jth column. N is the matrix size. $\delta = \{\delta_1, \delta_2, ..., \delta_N\}$, where $\delta_1 = 1$ and $\delta_i \in \{-1, 1\}$ for $2 \leq i \leq N$.

$$Perm(A) = (-1)^N \sum_{S \subseteq \{1,2,...,N\}} (-1)^{|S|} \prod_{i=1}^{N} \sum_{j \in S} a_{ij} \quad (1)$$

$$Perm(A) = \frac{\sum_{\delta} (\prod_{k=1}^{N} \delta_k) \prod_{i=1}^{N} \sum_{j=1}^{N} \delta_j a_{ij}}{2^{N-1}} \quad (2)$$

All programs we implement in this paper are for complex matrices. We can use them to test real matrices. The execution time is irrelevant to the matrix elements.

A. Speed performance

To test the upper-bound speed of computing permanents classically, we tried exploiting Tianhe-2's computing resources as many as possible (See Section IV and Appendix A). Tianhe-2 has 16,000 compute nodes, and each comprises two Intel Ivy Bridge Xeon E5 processors (CPUs) and three Xeon Phi coprocessors (denoted as MICs, because they adopt Intel Many Integrated Core architecture). Ryser's algorithm was tested with only CPUs, while BB/FG's algrithm was tested under two types of configurations: with only CPUs or with CPUs and MICs heterogeneously. We use real tests on small-scale subsystems (with ≤ 256 compute nodes) to evaluate and optimize our programs. Note that even a small-scale subsystem with 256 nodes still has a predicted LINPACK performance of 541.8 TeraFlops and a theoretical peak performance of 848.4 TeraFlops that may be ranked in the top 160 in Top500's list in Nov. 2015.

The key of gaining speedup from a parallel computer system is to implement the scalable parallel program, which can get more and more performance improvement with the increase of the computing resources. To evaluate the scalability of our programs, we tested them with different combinations of problem scale and parallel scale. According to the complexity ($O(2^N N^2)$, N is the matrix size), the number of operations almost grows double with the increase of N. Execution time grows by 1.95 times in FIG. 2(A), meaning that the additional cost of larger matrix is very small with the increase of problem scale. Meanwhile, execution time decreases with nearly linear speedup (slopes of 0.54 and 0.59 in FIG. 2(B)) when the parallel scale increases. Ideal slope is 0.5, meaning no additional cost. These suggest our programs have excellent scalability with only small and fixed cost from their serial parts.

The good scalability of our programs makes large-scale tests possible. We tested Ryser algorithms with the number of nodes ranging from 2,048 to 13,000. We found it became difficult for the large-scale system to complete execution of programs with long run time, because the system reliability became worse with the increase of processing units [36]. We also found some slow nodes prolonged the total execution time of programs sometimes. Take three tests on 46×46 matrices in TABLE I for ex-

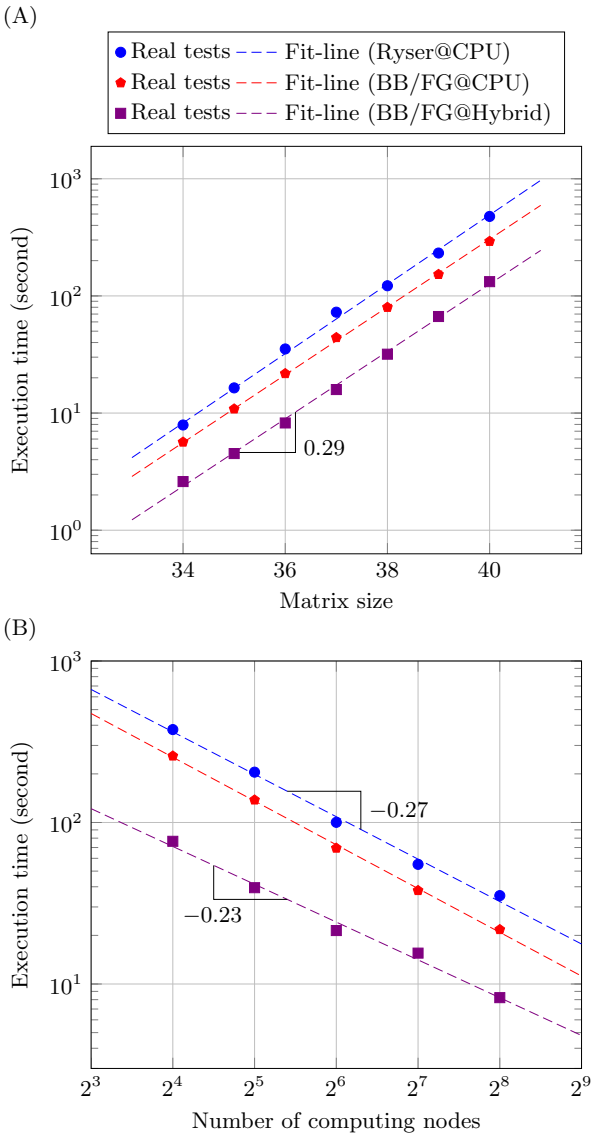

FIG. 2: **Execution times of computing permanents.** (A) Execution with varying matrix sizes and fixed system scale (a 256-node subsystem of Tianhe-2). "Ryser@CPU" denotes results of Ryser's algorithm running with only CPUs (MICs are not used); "BB/FG@CPU" denotes results of BB/FG's algorithm running with only CPUs; "BB/FG@Hybrid" denotes results of BB/FG's algorithm running with both CPUs and MICs. The slope of the fit-line for BB/FG@Hybrid means that execution times grow by $10^{0.29} = 1.95$ times with the increase of matrix sizes. (B) Execution with varying system scale and fixed matrix size (a 36×36 matrix). Execution times of Ryser@CPU (similar with BB/FG@CPU) decrease by $10^{-0.27} = 0.54$ times when number of compute nodes double, and those of BB/FG@Hybrid decrease by $10^{-0.23} = 0.59$ times.

ample. When the number of compute nodes grows from 4,096 to 8,192, execution time decreases to nearly the half. However, when the number of nodes grows from 8,192 to 13,000, execution time decreases a little, which exposes the existence of slow nodes. The 8,192 compute nodes has accounted for more than half nodes of Tianhe-2, and the 13,000 nodes 81.25%. These results show the largest problem scale (48×48-matrix) test and the largest parallel test (13000 compute nodes) with Tianhe-2.

TABLE I: **Large-scale real tests of Ryser's algorithm on Tianhe-2 supercomputer.** "# of Nodes" in the table indicates compute nodes of Tianhe-2, and "# of cores", CPU cores. Items in "Predicted time (s)" column are intervals of predicted execution time through fitting results of real tests with small-scale nodes. The blue items show that the execution time of real tests are out of the predicted intervals but quite close to the lower bound, mainly from the fluctuation of execution time. The red items show that the execution time is relatively too long, suggesting the existence of some slow nodes.

Matrix size	# of nodes	# of cores	Execution time (s)	Predicted time (s)
40	4,096	98,304	24.863563	[24.406, 30.566]
40	8,192	196,608	14.105145	[12.027, 15.262]
45	2,048	49,152	1967.7603	[2005.9, 2479.3]
45	4,096	98,304	984.02218	[988.44, 1237.9]
45	4,096	98,304	981.25833	[988.44, 1237.9]
45	4,096	98,304	986.09726	[988.44, 1237.9]
45	4,096	98,304	981.44862	[988.44, 1237.9]
45	13,000	312,000	450.62642	[303.97, 389.14]
46	4,096	98,304	2096.3798	[2065.7, 2587.1]
46	8,192	196,608	1054.9386	[1017.9, 1291.7]
46	13,000	312,000	1034.0247	[635.27, 813.25]
48	8,000	192,000	4630.0842	[4542.2, 5761.4]
48	8,000	192,000	4628.1068	[4542.2, 5761.4]
48	8,000	192,000	4657.8987	[4542.2, 5761.4]
48	8,000	192,000	4648.9111	[4542.2, 5761.4]
48	8,000	192,000	4627.6037	[4542.2, 5761.4]
48	8,192	196,608	4530.5931	[4433.5, 5626.1]
48	8,192	196,608	4498.4557	[4433.5, 5626.1]

To get the ideal upper-bound speed of Tianhe-2's full system, we fitted execution time of BB/FG's algorithm tested on small-scale systems, as shown in FIG. 3. Our fitting equation involved two parameters, matrix size and number of compute nodes (see Section IV and Appendix C). The fitting result suggests that the execution time for the whole system of Tianhe-2 to computing the permanent of a 50×50 matrix would be about 93.8 minutes, while the 95% confidence bound of this prediction is [77.41, 112.44] minutes.

B. Precision Performance

The precision issue comes from accumulated rounding errors introduced by limited word length of classical computers. We implemented Ryser's algorithm and BB/FG's algorithm with double-precision floating-point format (64 bits) of IEEE 754 standard. The total precision of a double-precision floating-point number is 53 bits, approximately 16 decimal digits ($53 \log_{10} 2 \approx 15.96$), because the fraction significand has 52 bits with an implicit bit in most cases. If no intermediate results in

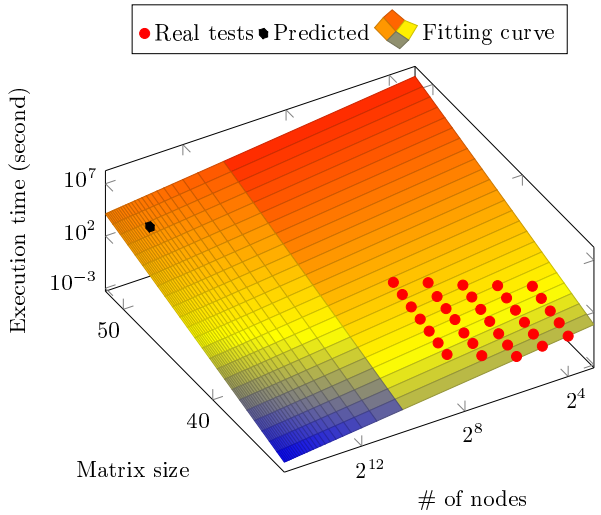

FIG. 3: **Fitting execution time of BB/FG's algorithm.** Data fitting is by the Curve Fitting Tool from MATLAB. The red points are the real tested data on the 256-node subsystem of Tianhe-2, and the black point is the predicted time used for the full system of Tianhe-2 (16,000 compute nodes: 32,000 CPUs and 48,000 MICs) to compute the permanent of a 50×50 matrix. The goodness of fitting is described by the following parameters: $SSE = 284.2$ (Sum of Squares for Error), which measures the deviation between the curve and the tested data; $R\_square = 0.994$, which indicates it to be a good fit when its value is close to 1, so is $Adjusted\ R\_square$, whose value is 0.9938 in our fitting, and $RMSE = 2.665$, which is similar to SSE.

the computational process are much larger than the final result, the accummulated errors will be marginal. Unfortunately, Ryser's algorithm may produce numbers, extremely larger than the final result. Thus, the errors of Ryser's algorithm may not be omitted sometimes. However, there is a division operation in the last step of BB/FG's algorithm as shown in Equation (2), which narrows the total error effciently. Therefore, the errors of BB/FG's algorithm is small. That means, BB/FG's algorithm is more trustable than Ryser's in terms of precision.

The accumulated rounding errors vary with different matrices. Here, we use a special kind of matrices to reveal the issue. Because the modulus of any element (a complex number) in a matrix for Boson sampling problem does not exceed 1, calculations of all-one matrices' (each element is 1) permanents in a special order produce the largest number possible (detailed in Appendix B 2). Namely, the errors for all-one matrix calculations give the upper bound of errors. Meanwhile, the permanent of an $N \times N$ all-one matrix is the factorial of N in theory, allowing us to verificate easily.

To evaluate errors of Ryser's algorithm and BB/FG's algorithm, we computed absolute errors and relative error rates of permanents of all-one matrices with different matrix sizes. We found the relative error rates of Ryser's algorithm was beyond 100% with ≥ 32 matrix sizes except small vibrations for 33×33 and 34×34 matrices as shown in FIG. 4(B). In FIG. 4, both errors of Ryser's algorithm and BB/FG's algorithm grow exponetially with the increase of matrix sizes according to the fitting lines, since the vertical axes used logarithmic scale. In FIG. 4(A), the absolute errors of Ryser's algorithm are $\times 10^7 \sim \times 10^9$ larger than that of BB/FG's algorithm, leading to the unacceptable relative error rates of Ryser's algorithm and the accurate one of BB/FG's algorithm (with the final division in Equation (2)). In FIG. 4(B), the fit-line predicts the relative error rate of BB/FG's algorithm for a 50×50 all-one matrix was about 0.0006%, and error rates does not beyond 10% when the dimensions are below 60×60. This shows that the precision issue overburdens Ryser's algorithm with large matrix size, and the smaller intermediate result and the last division saves BB/FG's algorithm. Our results suggest future research should use BB/FG's algorithm as a classical rival of quantum Boson sampling instead of Ryser's algorithm most considered before.

In practice, matrices are random leading to hard evaluation of their theoretical permanents. Fortunately, we can use a double check with both Ryser's algorithm and BB/FG's algorithm to mutually verify computation results. To examine the precision issue in more realistic situations, we generated three sets of random matrices: matrices corresponding to those each input (output) port of an interference network injects (ejects) one and only one Boson, matrices randomly derived from a 100×100 matrix, and matrices specially chosen to reveal errors more. In FIG. 5, we found the errors of random unitary matrices and derived matrices randomly chosen were marginal, but that of derived matrix specially chosen were still very large. The growing speed of errors of derived matrices specially chosen is as large as that of all-one matrices. This suggests a double check with both two algorithms is essential for future research to verify results produced by classical computers. Besides, the precision issue implicates quantum computation may outperforms classical computation not just in speed, but also in precision sometimes.

III. DISCUSSION

Tests of computing permanents on the most powerful classical computer is important for understanding the condition on which a quantum Boson sampling machine can surpass classical computation. Here we have shown tests both in speed and in precision on Tianhe-2 supercomputer, the fastest computer in the world now. Our tests show the upper-bound of computing the permanent using BB/FG's algorithm on Tianhe-2 supercomputer, and the precision issue of Ryser's algorithm, little known before. Limitted by testing conditions, the heterogeneous tests of the full system were not conducted. Our results still provide an important reference for experimental Boson sampling, although permanent calculation is not the complete simulation of Boson sampling. Because matrix permanents may approach 0, it is hard for us to give an

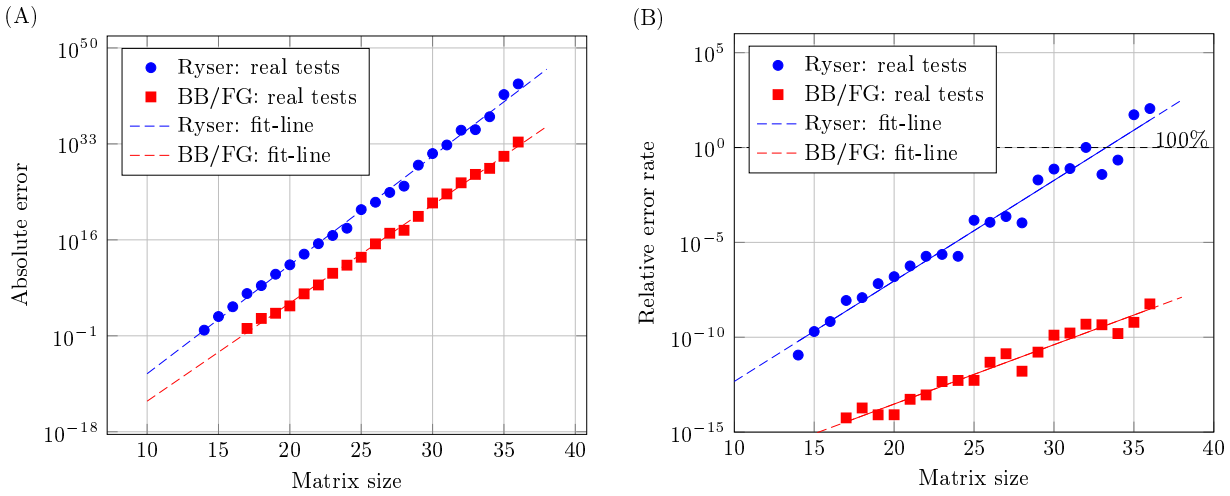

FIG. 4: **Errors of computing permanents of all-one matrices.** (A) An absolute error for an $N \times N$ all-one matrix is the difference between the value computed by Ryser's algorithm (BB/FG's algorithm) and the theoretical value of the permanent ($N!$). The theoretical value was computed by an arbitrary precision calculator. Ryser's algorithm has errors with the matrix sizes of ≥ 14, while BB/FG's algorithm has errors with the matrix sizes of ≥ 17. (B) The relative error rates are computed through dividing the absolute errors by the theoretical values. The relative error rate of Ryser's algorithm for a 32×32 all-one matrix achieves 100.95%, meaning the absolute error is as large as the permanent.

upper-bound of relative error rates. We only gave the upper bound of absolute error above. Overall, our results provide a reference from which we can know how large quantum Boson sampling machine can surpass current classical computational capacity and implies quantum computation outperforms classical computation not just in speed, but also in precision sometimes.

IV. METHODS

We developed the multi-level parallelism of the program based on the architecture of Tianhe-2 system. We parallelized the program at the level of the outer summation ($\sum_{S\subseteq\{1,2,\ldots,N\}}$ of Ryser's algorithm or $\sum_{\delta}$ of BB/FG's algorithm). The workload is distributed to the massive processes using `MPI`, and further distributed to the multiple threads within each process through `OpenMP` parallel library. We also implemented the heterogenous parallelism of the program: within one node, the workload was first divided into two parts according to a prefixed ratio, and distributed one to the process on MICs running in `offload` mode with the rest computed by the threads on CPUs. We optimized the programs through various means. The workload was balanced statically, and the part of program that running on MIC was rewritten with Single-Instruction-Multi-Data (SIMD) instructions to make full use of the Vector Process Unit (VPU) of MICs. (See Appendix A for more details)

The fitting curve in FIG. 3 is conducted with MATLAB, and the fitting equation is shown in Equation (3) (See Appendix C for more details).

$$T = \frac{9.805N^2 2^N}{n^{0.8782} \times 10^{12}} \tag{3}$$

where T represents the execution time, N is the size of the matrix and n is the number of nodes used for the simulation.

V. ACKNOWLEDGEMENTS

We gratefully acknowledge the help from the National Supercomputer Center in Guangzhou. We also appreciate the helpful discussion with Xun Yi, Xuan Zhu, Jiangfang Ding, Hongjuan He, Yingwen Liu, Dongyang Wang and Shichuan Xue. This work was supported by the National Natural Science Foundation of China (NSFC) No. 61221491, and the Open Fund from HPCL No.201401-01.

[1] Deutsch, D. Quantum theory, the church-turing principle and the universal quantum computer. *Proceedings of the Royal Society of London A: Mathematical, Physical and Engineering Sciences* **400**(1818), 97–117 (1985).

[2] Nielsen, M. A. and Chuang, I. L. *Quantum Computation and Quantum Information: 10th Anniversary Edition*. Cambridge University Press, New York, NY, USA, 10th edition, (2011).

[3] Shor, P. W. Algorithms for quantum computation: discrete logarithms and factoring. In *Foundations of Computer Science, 1994 Proceedings., 35th Annual Symposium on*, 124–134, , Nov

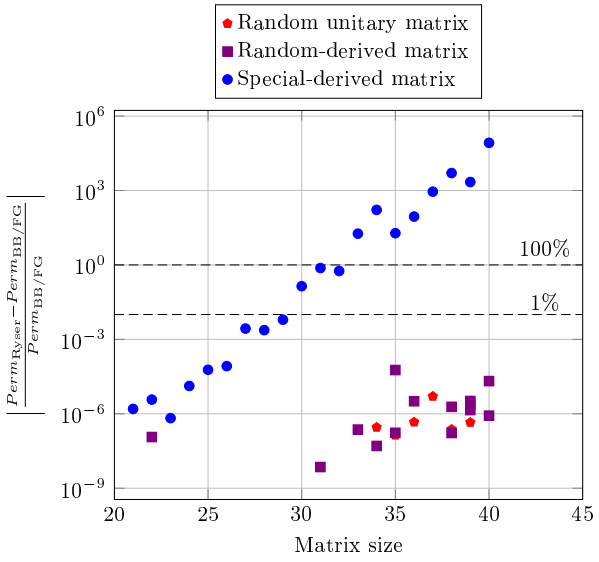

FIG. 5: **Errors of computing permanents of random matrices.** $Perm_{\mathrm{Ryser}}$ ($Perm_{\mathrm{BB/FG}}$) denotes the value of permanent caculated through Ryser's (BB/FG's) algorithm. "Random unitary matrix" denotes results of matrices corresponding to that each input (output) port of an interference network injects (ejects) one and only one Boson. "Random-derived matrix" denotes results of matrices randomly derived from a 100×100 matrix, and "Special-derived matrix" denotes results of matrices specially chosen to reveal errors more. Two algorithms give very similar results for two former matrices. However, the special-derived matrices are still overburdened by accumulated rounding errors. The relative difference between two algorithms achieves 13.9% for the 30×30 special-derived matrix tested.

(1994).

[4] Martin-Lopez, E., Laing, A., Lawson, T., Alvarez, R., Zhou, X.-Q., and O'Brien, J. L. Experimental realization of shor's quantum factoring algorithm using qubit recycling. *Nat Photon* **6**(11), 773–776, 11 (2012).

[5] Griffiths, R. B. and Niu, C.-S. Semiclassical fourier transform for quantum computation. *Phys. Rev. Lett.* **76**, 3228–3231, Apr (1996).

[6] Kaliski, B. TWIRL and RSA key size. http://www.emc.com/emc-plus/rsa-labs/historical/twirl-and-rsa-key-size.htm, (2003).

[7] Lanyon, B. P., Weinhold, T. J., Langford, N. K., Barbieri, M., James, D. F. V., Gilchrist, A., and White, A. G. Experimental demonstration of a compiled version of shor's algorithm with quantum entanglement. *Phys. Rev. Lett.* **99**, 250505, Dec (2007).

[8] Politi, A., Matthews, J. C. F., and O'Brien, J. L. Shor's quantum factoring algorithm on a photonic chip. *Science* **325**(5945), 1221–1221 (2009).

[9] Parker, S. and Plenio, M. B. Efficient factorization with a single pure qubit and log$N$ mixed qubits. *Phys. Rev. Lett.* **85**, 3049–3052, Oct (2000).

[10] Lu, C.-Y., Browne, D. E., Yang, T., and Pan, J.-W. Demonstration of a compiled version of shor's quantum factoring algorithm using photonic qubits. *Phys. Rev. Lett.* **99**, 250504, Dec (2007).

[11] Aaronson, S. and Arkhipov, A. The computational complexity of linear optics. In *Proceedings of the Forty-third Annual ACM Symposium on Theory of Computing*, STOC '11, 333–342 (ACM, New York, NY, USA, 2011).

[12] Scheel, S. Permanents in linear optical networks. *eprint arXiv* **quant-ph/0406127**, June (2004).

[13] Spring, J. B., Metcalf, B. J., Humphreys, P. C., Kolthammer, W. S., Jin, X.-M., Barbieri, M., Datta, A., Thomas-Peter, N., Langford, N. K., Kundys, D., Gates, J. C., Smith, B. J., Smith, P. G. R., and Walmsley, I. A. Boson sampling on a photonic chip. *Science* **339**(6121), 798–801 (2013).

[14] Broome, M. A., Fedrizzi, A., Rahimi-Keshari, S., Dove, J., Aaronson, S., Ralph, T. C., and White, A. G. Photonic Boson sampling in a tunable circuit. *Science* **339**(6121), 794–798 (2013).

[15] Tillmann, M., Dakic, B., Heilmann, R., Nolte, S., Szameit, A., and Walther, P. Experimental Boson sampling. *Nat Photon* **7**(7), 540–544, 07 (2013).

[16] Crespi, A., Osellame, R., Ramponi, R., Brod, D. J., Galvao, E. F., Spagnolo, N., Vitelli, C., Maiorino, E., Mataloni, P., and Sciarrino, F. Integrated multimode interferometers with arbitrary designs for photonic Boson sampling. *Nat Photon* **7**(7), 545–549, 07 (2013).

[17] Aaronson, S. Scattershot Bosonsampling: A new approach to scalable Bosonsampling experiments. http://www.scottaaronson.com/blog/?p=1579, (2013).

[18] Lund, A. P., Laing, A., Rahimi-Keshari, S., Rudolph, T., O'Brien, J. L., and Ralph, T. C. Boson sampling from a gaussian state. *Phys. Rev. Lett.* **113**, 100502, Sep (2014).

[19] Bentivegna, M., Spagnolo, N., Vitelli, C., Flamini, F., Viggianiello, N., Latmiral, L., Mataloni, P., Brod, D. J., Galvão, E. F., Crespi, A., Ramponi, R., Osellame, R., and Sciarrino, F. Experimental scattershot Boson sampling. *Science Advances* **1**(3) (2015).

[20] Motes, K. R., Gilchrist, A., Dowling, J. P., and Rohde, P. P. Scalable Boson sampling with time-bin encoding using a loop-based architecture. *Phys. Rev. Lett.* **113**, 120501, Sep (2014).

[21] Spring, J. B., Mennea, P. L., Metcalf, B. J., Humphreys, P. C., Gates, J. C., Rogers, H. L., Soeller, C., Smith, B. J., Kolthammer, W. S., Smith, P. G. R., and Walmsley, I. A. A chip-based array of near-identical, pure, heralded single photon sources. *ArXiv e-prints* **1603.06984**, March (2016).

[22] Carolan, J., Harrold, C., Sparrow, C., Martín-López, E., Russell, N. J., Silverstone, J. W., Shadbolt, P. J., Matsuda, N., Oguma, M., Itoh, M., Marshall, G. D., Thompson, M. G., Matthews, J. C. F., Hashimoto, T., O'Brien, J. L., and Laing, A. Universal linear optics. *Science* **349**(6249), 711–716 (2015).

[23] Defienne, H., Barbieri, M., Walmsley, I. A., Smith, B. J., and Gigan, S. Two-photon quantum walk in a multimode fiber. *Science Advances* **2**(1) (2016).

[24] Rohde, P. P. and Ralph, T. C. Error tolerance of the Boson-sampling model for linear optics quantum computing. *Phys. Rev. A* **85**, 022332, Feb (2012).

[25] Rohde, P. P. Optical quantum computing with photons of arbitrarily low fidelity and purity. *Phys. Rev. A* **86**, 052321, Nov (2012).

[26] Rahimi-Keshari, S., Ralph, T. C., and Caves, C. M. Efficient classical simulation of quantum optics. *ArXiv e-prints* **1511.06526**, November (2015).

[27] Motes, K. R., Dowling, J. P., and Rohde, P. P. Spontaneous parametric down-conversion photon sources are scalable in the asymptotic limit for Boson sampling. *Phys. Rev. A* **88**, 063822, Dec (2013).

[28] Motes, K. R., Dowling, J. P., Gilchrist, A., and Rohde, P. P. Implementing Bosonsampling with time-bin encoding: Analysis of loss, mode mismatch, and time jitter. *Phys. Rev. A* **92**, 052319, Nov (2015).

[29] Aaronson, S. and Arkhipov, A. Bosonsampling is far from uniform. *Quantum Info. Comput.* **14**(15-16), 1383–1423, November (2014).

[30] Spagnolo, N., Vitelli, C., Bentivegna, M., Brod, D. J., Crespi, A., Flamini, F., Giacomini, S., Milani, G., Ramponi, R., Mataloni, P., Osellame, R., Galvao, E. F., and Sciarrino, F. Experimental validation of photonic Boson sampling. *Nat Photon* **8**(8), 615–620, 08 (2014).

[31] Wang, S.-T. and Duan, L.-M. Certification of Boson Sampling

Devices with Coarse-Grained Measurements. *ArXiv e-prints* **1601.02627**, January (2016).
[32] Rohde, P. P., Motes, K. R., Knott, P. A., Fitzsimons, J., Munro, W. J., and Dowling, J. P. Evidence for the conjecture that sampling generalized cat states with linear optics is hard. *Phys. Rev. A* **91**, 012342, Jan (2015).
[33] Seshadreesan, K. P., Olson, J. P., Motes, K. R., Rohde, P. P., and Dowling, J. P. Boson sampling with displaced single-photon fock states versus single-photon-added coherent states: The quantum-classical divide and computational-complexity transitions in linear optics. *Phys. Rev. A* **91**, 022334, Feb (2015).
[34] Olson, J. P., Seshadreesan, K. P., Motes, K. R., Rohde, P. P., and Dowling, J. P. Sampling arbitrary photon-added or photon-subtracted squeezed states is in the same complexity class as Boson sampling. *Phys. Rev. A* **91**, 022317, Feb (2015).
[35] Liao, X., Xiao, L., Yang, C., and Lu, Y. Milkyway-2 supercomputer: System and application. *Front. Comput. Sci.* **8**(3), 345–356, June (2014).
[36] Yang, X., Wang, Z., Xue, J., and Zhou, Y. The reliability wall for exascale supercomputing. *IEEE Transactions on Computers* **61**(6), 767–779, June (2012).

Appendix A: Methodology (Parallelization and Optimization)

We paralleled and optimized the programs of Ryser's algorithm and BB/FG's algorithm on Tianhe-2 supercomputer [1]. The architecture of Tianhe-2 is shown in FIG. A1 and FIG. A2. The performance parameters of Tianhe-2 is listed in TABLE AI.

1. Utilizing Multiple CPUs (and CPU cores)

We implemented the parallelism of these two algorithms in Equation (1) and Equation (2) based on `MPI` (for utilizing multiple CPUs) and `OpenMP` (for utilizing multiple CPU cores) libraries. The parallelized Ryser's algorithm is shown in Algorithm 1. The initialization set ID for each process, after which the main process generate the matrix and broadcast the data to other processes through `MPI` library. The length of the original loop is divided into several segments according to the number of processes. Each process takes different segments as the loop section. The loop would be executed using `OpenMP` libraries by multi-threads. Processes totally have no data dependency except the final $ALLREDUCE$ operation in which the main process gathers data from all the other process. Except this data gathering, no synchronization is needed. The parallelized BB/FG's algorithm is similar except the iteration body, the total length of the main loop (reduced to 2^{N-1}) and the final division operation, as shown in Algorithm 2.

2. Load Balance

We optimized the parallelized Ryser's algorithm through load balance. In Algorithm 1, within the calculation of $\sum_{j\in S} a_{ij}$, the times of addition is related to $|S|$. This leads an imbalance loads. Therefore, we designed a optimizing algorithm with load balance, as Algorithm 3 shows. The variable $temp$ is just the N-bit 1's complement of $iter$. However, BB/FG's algorithm is free from the imbalance problem because each iteration in the loop of Algorithm 2 always performs N times additions/substractions.

Algorithm 1 Parallelized Ryser's algorithm

Require: Matrix: A;Scale of the matrix: N; Number of nodes: $size$
Ensure: Permanent of A: $Perm$
INITIAL();
if $rank == 0$ **then**
  Generate matrix;
  Broadcast data to all other process;
end if
$length = \frac{2^N-1}{\#\ of\ processes}$
$start = rank * length$
$end = start + length$
for $iter = start$ to end **do**
  Convert $iter$ to the set S;
  Calculate $\sum_{j\in S} a_{ij}$ for each row;
  Multiply the sum of each row into a product: $\prod_{i=1}^{N} \sum_{j\in S} a_{ij}$;
  if $|S|$ is odd **then**
    $Perm = Perm - delta$;
  else
    $Perm = Perm + delta$;
  end if
end for
ALLREDUCE($Perm$);
if N is odd **and** $rank == 0$ **then**
  $Perm = -1 * Perm$;
end if

3. Utilizing both CPUs and MICs

We implemented the heterogeneous parallelism of BB/FG's algorithm among CPUs and MICs with two steps. The first step is to rewrite BB/FG's algorithm with SIMD instructions to take advantages of the VPU(Vector Process Unit) in MIC as shown in Algorithm 4, which makes full use of MICs. Data are loaded into vector registers before calculation, the variables with prefix "_" represents the vector variables, which would be stored in the vector registers in the VPU. The second step is to implement the heterogeneous parallelism between CPUs and MICs as shown in Algorithm 5.

Appendix B: Detailed Real Test Data

1. Speed Performance

TABLE AII and TABLE AIII show the detailed real test data of Ryser's algorithm and BB/FG's algorithm

Algorithm 2 Parallelized BB/FG's algorithm

Require: Matrix: A;Scale of the matrix: N; Number of nodes: $size$
Ensure: Permanent of A: $Perm$
INITIAL();
if $rank == 0$ **then**
  Generate matrix;
  Broadcast data to all other process;
end if
$length = \frac{2^{(N-1)}-1}{\#\ of\ processes}$
$start = rank * length$
$end = start + length$
for $iter = 0$ to $length$ **do**
  Convert $iter$ to the set δ, δ_i is 1 when the i^{th} bit in iter is 1, -1 otherwise;
  Calculate $s_j = \sum_{i=1}^{N} \delta_i a_{ij}$ for j in {1,2,...,N};
  Calculate $delta = \prod_{j=1}^{N} s_j$;
  if The number of -1 in δ is odd **then**
    $Perm = Perm - delta$;
  else
    $Perm = Perm + delta$;
  end if
end for
ALLREDUCE($Perm$);
if N is odd **and** $rank == 0$ **then**
  $Perm = \frac{Perm}{2^{N-1}}$;
end if

Algorithm 3 Ryser's algorithm with load balance

Initializing;
$length = 2^{N-1} - 1$;
$start = rank * length$;
$end = start + end$;
for $iter = start$ to end **do**
  Compute $(-1)^{|S|} \prod_{i=1}^{N} \sum_{j \in S} a_{ij}$ corresponding to $iter$;
  $temp = 2^N - iter - 1$;
  Compute $(-1)^{|S|} \prod_{i=1}^{N} \sum_{j \in S} a_{ij}$ corresponding to $temp$;
end for

respectively. Some of data in these tables are used in FIG. 2 and FIG. 3.

Some screenshots and a photograph are shown here. FIG. A3 and FIG. A4 are screenshots in which Tianhe-2 was computing the permanent of a 45×45 matrix. FIG. A5 shows an error case in which some node failed during the execution.

2. Precision Performance

TABLE AIV $\sim$ TABLE AVII show the detailed real test errors of BB/FG's algorithm and Ryser's algorithm. TABLE AIV and TABLE AVI show results for real matrices, and some of data are used in FIG. 4. TABLE AV and TABLE AVII show results for complex matrices.

Different order of addition would produce different intermediate results, whose rounding error are also different. Thus the order of addition in Ryser's algorithm could affect the precision badly. We tested some different order of addition, and list the errors. The result is shown in TABLE AVIII. Taking $N = 3$ as the example, the compute length is 8. In original order, the order of summation is: $0-1+2-3+4-5+6-7$, where the numbers denotes the order of loop represented by variable $iter$ in Algorithm 1. In random order, the summation order is decided randomly; in merge, the order of summation is:

Algorithm 4 Vectorized BB/FG's algorithm on MIC

Require: Matrix: A;Scale of the matrix: N;
Ensure: Permanent of A: $Perm$
$length = 2^{N-1} - 1$;
for $iter = 0$ to $length$ **do**
  $\_R$ =**Load**(A);
  for $itx = 1$ to N **do**
    $\_A$ =**Load**($A + itx * N$);
    if $iter >> (itx - 1)\&1$ **then**
      $\_R+ = \_A$;
    else
      $\_R- = \_A$;
    end if
  end for
  for $itx = 1$ to $N/VECSIZE$ **do**
    $\_R2$ =**Load**($A + itx * VECSIZE$);
    for $ity = 1$ to N **do**
      $\_A$ =**Load**($A + itx * VECSIZE + ity * N$);
      if $iter >> (itx - 1)\&1$ **then**
        $\_R2+ = \_A$;
      else
        $\_R2- = \_A$;
      end if
    end for
    $\_R = \_R * \_R2$;
  end for
  if The number of -1 in δ is odd **then**
    $Perm = Perm - delta$;
  else
    $Perm = Perm + delta$;
  end if
end for
$Perm = \frac{Perm}{2^{N-1}}$;

Algorithm 5 Heterogenous BB/FG's algorithm

Require: Matrix: A; Scale of the matrix: N; Number of processes: $size$;
Ensure: Permanent of A: $Perm$
$INITIAL(size, rank)$; // $rank$ is the ID of the process
$TotalLength = 2^{N-1} - 1$;
Decide the computing section of each process;
Decide the computing section of CPUs and MICs according to the pre-fixed $ratio$;
$MIC\_Computing(MIC\_Section)$;
$Host\_Computing(CPU\_Section)$;
Host Waits the data from the MICs;
ALLREDUCE($Perm$);
if N is odd **and** $rank == 0$ **then**
  $Perm = \frac{Perm}{2^{N-1}}$;
end if

$(((0-1)+(2-3))+((4-5)+(6-7)))$, thus the neighbouring numbers were summed up first, which is much like a tree structure. in the separate operation, the order of summation is $(0+2+4+6)-(1+3+5+7)$.

TABLE AIX, TABLE AX and TABLE AXI show the detailed real test errors for random matrices, and some of data are used in FIG. 5.

Appendix C: Fitting Equation

The execution time in the fitting curve in FIG. 3 is modeled as T in Equation (A1).

$$T = aN^2 2^N n^b \tag{A1}$$

where N stands for the size of matrix, n is the number of compute nodes, and a together with b are the fitting coefficients. The part of $N^2 2^N$ comes from the complexity of BB/FG's algorithm, $O(N^2 2^N)$. In the parallelized algorithm, computing tasks are allocated to multiple compute nodes. Therefore, we add the number of compute nodes in the equation. We conducted the curve fitting with MATLAB and the fitting result is shown in TABLE AXII.

[1] Liao, X., Xiao, L., Yang, C., and Lu, Y. Milkyway-2 supercomputer: System and application. *Frontiers of Computer Science* **8**(3), 345–356, June (2014).

[2] Yang, X., Wang, Z., Xue, J., and Zhou, Y. The reliability wall for exascale supercomputing. *IEEE Transactions on Computers* **61**(6), 767–779, June (2012).

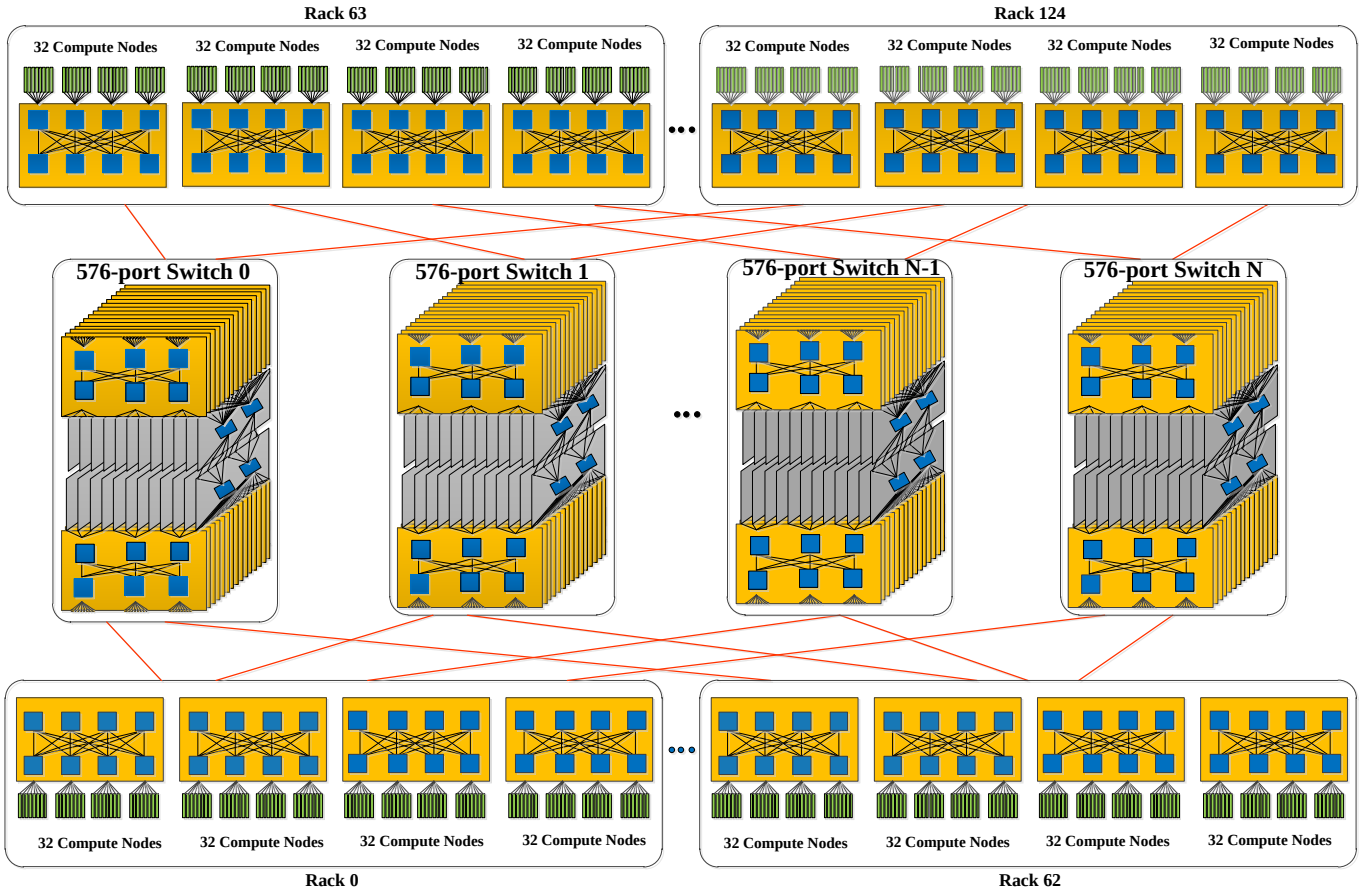

FIG. A1: **The architecture of Tianhe-2 supercomputer [1].** Each rack contains 128 compute nodes. Each rack is connected to the 576-port switch. The high performance network ensures the efficiency of the parallelism of the applications.

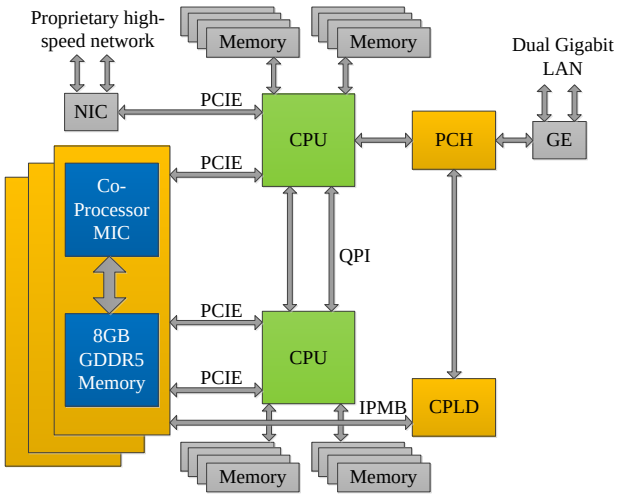

FIG. A2: **The architecture of a node in Tianhe-2 supercomputer [1].** Each node comprises 2 CPUs and 3 MIC coprocessor.

TABLE AI: Performance Parameters of Tianhe-2 Supercomputer

Item		Parameters of a node	Parameters of the System
Peak Performance		3.43 TeraFlops	54.90 PetaFlops
Processor	Intel Xeon E5 (12 cores)	2 (24 cores)	32,000 (384 thousand cores)
	Xeon Phi (57 cores)	3 (171cores)	48,000 (2.736 million Cores)
Memory Storage Capacity		64GB+8GB (Xeon Phi)	1.408PB
Disk Capacity		12.4PB	
Mainboard (Two compute nodes)		8,000	
Front-Ending Processor FT-1500(16 cores)		4,096	
Interconnect Network		TH Express-2	
Operating System		Kylin	
Power Consumption		24 MW (17.808 MW without cooling system)	

TABLE AII: **Execution time of Ryser's algorithm (with only CPUs).** The data of "Ryser@CPU" in FIG. 2 come from this table. "# of Nodes" in the table indicates the number of compute nodes used. "Size of Matrix" is the problem scale tested. Items in "Time (s)" represent the execution time used for the computation, in the unit of second.

# of Nodes	Size of Matrix	Time (s)	# of Nodes	Size of Matrix	Time (s)	# of Nodes	Size of Matrix	Time (s)
1	25	2.0345	2	26	1.8804	4	27	2.5416
1	26	3.8637	2	27	4.1826	4	28	4.7559
1	27	6.9495	2	28	9.0362	4	29	9.3383
1	28	14.971	2	29	15.790	4	30	18.031
1	29	30.954	2	30	33.261	4	31	39.437
1	30	66.364	2	31	69.945	4	32	75.537
1	31	150.20	2	32	149.75	4	33	157.01
8	28	2.6874	16	29	2.8091	32	30	3.1978
8	29	5.2117	16	30	5.5132	32	31	6.4735
8	30	9.2390	16	31	10.633	32	32	13.331
8	31	19.593	16	32	26.266	32	33	22.863
8	32	42.515	16	33	42.930	32	34	47.566
8	33	81.848	16	34	88.225	32	35	92.872
8	34	167.40	16	35	173.84	32	36	192.74
64	31	3.3718	128	32	3.5943	256	33	3.6789
64	32	6.2294	128	33	6.9304	256	34	7.5186
64	33	13.250	128	34	13.682	256	35	15.307
64	34	27.241	128	35	29.046	256	36	30.396
64	35	59.270	128	36	48.754	256	37	62.923
64	36	101.08	128	37	102.13	256	38	110.22
64	37	186.23	128	38	193.55	256	39	209.22

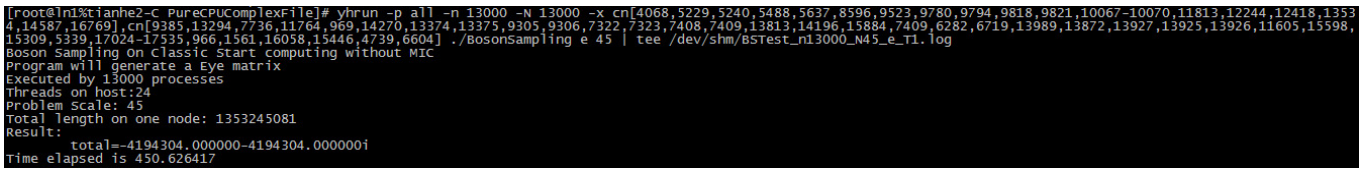

FIG. A3: **Screenshot of computing the permanent of a** 45×45 **matrix on 13,000 nodes.** The command line is "yhrun -p all -n 13000 -N 13000 -x cn[4068...6604] ./BosonSampling e 45 | tee /dev/shm/BSTest_n13000_N45_e_T1.log", where "yhrun" is the command to submit the task, "-p all" means the program would be executed on all the partition of Tianhe-2, "-n 13000 -N 13000" means we would start 13,000 processes on 13,000 compute nodes, "-x cn[4068...6604]" defines the nodes that we won't use for this computation and "./BosonSampling e 45" shows the input is a 45×45-matrix with diagonal elements to be $1 + i$ and other elements to be 0. The output would be recorded in file "/dev/shm/BSTest_n13000_N45_e_T1.log". The line after "Result:" gives the computing result, which equals to the theoretical value $(1 + i)^{45}$, and the last line gives the execution time.

TABLE AIII: **Execution time of heterogenous BB/FG's algorithm (with both CPUs and MICs).** The data of "BB/FG@Hybrid" in FIG. 2 and the fitting data in FIG. 3 come from this table. "# of Nodes" in the table indicates compute nodes of Tianhe-2, "Size of Matrix" is the problem scale tested. Items in "Time (s)" represent the execution time used for the computation, in the unit of second.

# of Nodes	Size of Matrix	Time (s)	# of Nodes	Size of Matrix	Time (s)	# of Nodes	Size of Matrix	Time (s)
1	24	0.7499	2	25	1.0282	4	26	1.0350
1	25	1.1063	2	26	1.1088	4	27	1.5203
1	26	1.3669	2	27	1.3720	4	28	1.3382
1	27	1.7670	2	28	1.7178	4	29	2.4851
1	28	3.7542	2	29	3.8401	4	30	2.6999
1	29	7.0984	2	30	4.4428	4	31	7.4401
1	30	13.970	2	31	14.294	4	32	8.9424
1	31	28.081	2	32	16.793	4	33	36.460
1	32	55.677	2	33	72.983	4	34	57.598
8	27	1.3791	16	28	1.3742	32	29	1.3799
8	28	1.5570	16	29	1.5762	32	30	1.6045
8	29	1.8099	16	30	1.8922	32	31	1.9624
8	30	2.5298	16	31	2.6100	32	32	2.7685
8	31	4.0341	16	32	3.7448	32	33	5.4228
8	32	6.2521	16	33	9.5439	32	34	9.9724
8	33	18.486	16	34	17.642	32	35	19.550
8	34	31.097	16	35	38.580	32	36	39.477
8	35	76.571	16	36	76.492	32	37	80.358
64	30	1.3939	128	31	1.4278	256	32	1.6232
64	31	1.5781	128	32	1.9457	256	33	1.9047
64	32	1.9385	128	33	2.1552	256	34	2.6021
64	33	3.3056	128	34	4.3292	256	35	4.5121
64	34	5.4466	128	35	5.9397	256	36	8.2317
64	35	11.228	128	36	15.533	256	37	15.877
64	36	21.428	128	37	23.652	256	38	31.815
64	37	44.767	128	38	46.065	256	39	66.710
64	38	84.098	128	39	133.18	256	40	132.35

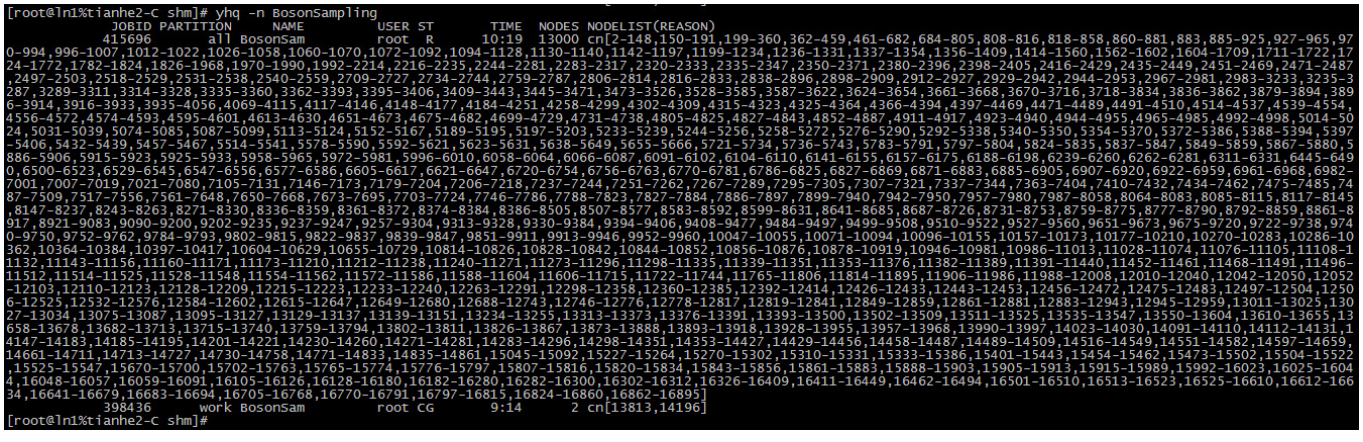

FIG. A4: **Screenshot of the node list of the 13,000 nodes used.** The command line is "yhq -n BosonSampling", which output the job with the executive named "BosonSampling" in the job sequence, the partition where this job was allocated and above all, the node list of this job.

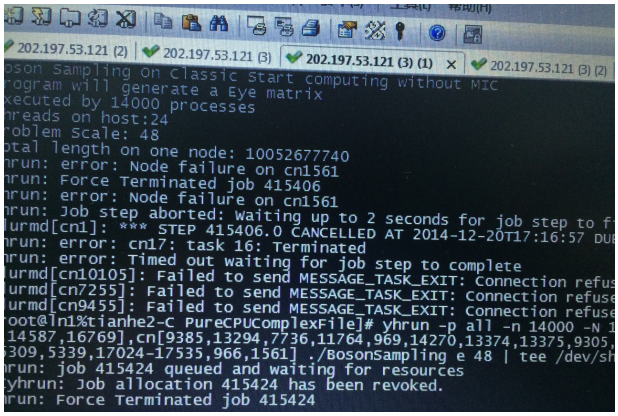
202.197.53.121 (2)
202.197.53.121 (3)
202.197.53.121 (3) (1)
202.197.53.121 (3) (2)
oson Sampling On Classic Start computing without MIC
rogram will generate a Eye matrix
xecuted by 14000 processes
hreads on host:24
roblem Scale: 48
otal length on one node: 10052677740
hrun: error: Node failure on cn1561
hrun: Force Terminated job 415406
hrun: error: Node failure on cn1561
hrun: Job step aborted: Waiting up to 2 seconds for job step to f
lurmd[cn1]: *** STEP 415406.0 CANCELLED AT 2014-12-20T17:16:57 DU
hrun: error: cn17: task 16: Terminated
hrun: error: Timed out waiting for job step to complete
lurmd[cn10105]: Failed to send MESSAGE_TASK_EXIT: Connection refus
lurmd[cn7255]: Failed to send MESSAGE_TASK_EXIT: Connection refuse
lurmd[cn9455]: Failed to send MESSAGE_TASK_EXIT: Connection refuse
oot@ln1%tianhe2-C PureCPUComplexFile]# yhrun -p all -n 14000 -N 1
14587,16769],cn[9385,13294,7736,11764,969,14270,13374,13375,9305,
309,5339,17024-17535,966,1561] ./BosonSampling e 48 | tee /dev/sh
hrun: job 415424 queued and waiting for resources
yhrun: Job allocation 415424 has been revoked.
hrun: Force Terminated job 415424

FIG. A5: **Photograph that shows error occurred during the computation on 14,000 nodes** Errors occurred more frequently when the number of nodes increases [2]. In this photograph, the node cn1561 failed during the execution, leading to the job termination and more errors in the node communication.

TABLE AIV: **Errors of BB/FG's algorithm for real matrices.** Some data in FIG. 4 come from this table. We did the precision test by computing the permanent of an $N \times N$ all-r real matrix, in which each element has a real value of r ("Value of Elements"). In this case, the ideal permanent is $r^N \cdot N!$ ("Theor. Value"), where N is the size of the matrix ("Size of Matrix"). "Comput. Value" is the result produced by BB/FG's algorithm. The "Abs. Error" is the absolute difference between the computing value and the theoretical value, and "Relative Error Rate" is the relative error rate.

Size of Matrix	Value of Elements	Comput. Value	Theor. Value	Abs. Error	Relative Error Rate	Value of Elements	Comput. Value	Theor. Value	Abs. Error	Relative Error Rate
17	1	3.56E+14	3.56E+14	2.00E+00	5.62E-15	0.1	3.56E-03	3.56E-03	3.64E-17	1.02E-14
18	1	6.40E+15	6.40E+15	1.20E+02	1.87E-14	0.1	6.40E-03	6.40E-03	2.78E-16	4.35E-14
19	1	1.22E+17	1.22E+17	9.92E+02	8.15E-15	0.1	1.22E-02	1.22E-02	1.18E-15	9.67E-14
20	1	2.43E+18	2.43E+18	2.00E+04	8.21E-15	0.1	2.43E-02	2.43E-02	4.25E-15	1.75E-13
21	1	5.11E+19	5.11E+19	2.74E+06	5.36E-14	0.1	5.11E-02	5.11E-02	4.36E-15	8.54E-14
22	1	1.12E+21	1.12E+21	1.02E+08	9.11E-14	0.1	1.12E-01	1.12E-01	6.60E-14	5.87E-13
23	1	2.59E+22	2.59E+22	1.20E+10	4.63E-13	0.1	2.59E-01	2.59E-01	1.06E-13	4.08E-13
24	1	6.20E+23	6.20E+23	3.27E+11	5.28E-13	0.1	6.20E-01	6.20E-01	7.66E-13	1.23E-12
25	1	1.55E+25	1.55E+25	8.28E+12	5.34E-13	0.1	1.55E+00	1.55E+00	4.33E-12	2.79E-12
26	1	4.03E+26	4.03E+26	1.94E+15	4.81E-12	0.1	4.03E+00	4.03E+00	7.01E-12	1.74E-12
27	1	1.09E+28	1.09E+28	1.47E+17	1.35E-11	0.1	1.09E+01	1.09E+01	8.24E-11	7.57E-12
28	1	3.05E+29	3.05E+29	4.95E+17	1.62E-12	0.1	3.05E+01	3.05E+01	2.18E-10	7.15E-12
29	1	8.84E+30	8.84E+30	1.45E+20	1.64E-11	0.1	8.84E+01	8.84E+01	2.76E-09	3.12E-11
30	1	2.65E+32	2.65E+32	3.42E+22	1.29E-10	0.1	2.65E+02	2.65E+02	4.66E-09	1.76E-11
31	1	8.22E+33	8.22E+33	1.37E+24	1.67E-10	0.1	8.22E+02	8.22E+02	5.54E-08	6.73E-11
32	1	2.63E+35	2.63E+35	1.28E+26	4.87E-10	0.1	2.63E+03	2.63E+03	9.49E-07	3.61E-10
33	1	8.68E+36	8.68E+36	3.95E+27	4.55E-10	0.1	8.68E+03	8.68E+03	3.12E-07	3.60E-11
34	1	2.95E+38	2.95E+38	4.64E+28	1.57E-10	0.1	2.95E+04	2.95E+04	1.25E-05	4.25E-10
35	1	1.03E+40	1.03E+40	6.32E+30	6.12E-10	0.1	1.03E+05	1.03E+05	1.32E-04	1.28E-09
36	1	3.72E+41	3.72E+41	2.13E+33	5.72E-09	0.1	3.72E+05	3.72E+05	1.70E-03	4.56E-09
17	10	3.56E+31	3.56E+31	6.98E+17	1.96E-14	0.2	466.2066	466.2066	3.98E-12	8.53E-15
18	10	6.40E+33	6.40E+33	1.11E+20	1.73E-14	0.2	1678.344	1678.344	6.62E-11	3.94E-14
19	10	1.22E+36	1.22E+36	2.01E+22	1.65E-14	0.2	6377.707	6377.707	6.37E-10	9.98E-14
20	10	2.43E+38	2.43E+38	4.99E+24	2.05E-14	0.2	25510.83	25510.83	4.34E-09	1.70E-13
21	10	5.11E+40	5.11E+40	1.86E+27	3.63E-14	0.2	107145.5	107145.5	6.05E-09	5.65E-14
22	10	1.12E+43	1.12E+43	4.23E+29	3.77E-14	0.2	471440.1	471440.1	2.95E-07	6.25E-13
23	10	2.59E+45	2.59E+45	3.28E+32	1.27E-13	0.2	2168624	2168624	7.00E-07	3.23E-13
24	10	6.20E+47	6.20E+47	7.70E+35	1.24E-12	0.2	10409397	10409397	1.49E-05	1.43E-12
25	10	1.55E+50	1.55E+50	3.87E+38	2.50E-12	0.2	52046984	52046984	2.18E-04	4.19E-12
26	10	4.03E+52	4.03E+52	4.48E+40	1.11E-12	0.2	2.71E+08	2.71E+08	1.96E-04	7.22E-13
27	10	1.09E+55	1.09E+55	7.44E+43	6.84E-12	0.2	1.46E+09	1.46E+09	1.09E-02	7.44E-12
28	10	3.05E+57	3.05E+57	4.22E+46	1.38E-11	0.2	8.18E+09	8.18E+09	1.11E-01	1.36E-11
29	10	8.84E+59	8.84E+59	1.07E+50	1.21E-10	0.2	4.75E+10	4.75E+10	8.67E-01	1.83E-11
30	10	2.65E+62	2.65E+62	1.67E+52	6.31E-11	0.2	2.85E+11	2.85E+11	2.53E+01	8.87E-11
31	10	8.22E+64	8.22E+64	1.27E+55	1.55E-10	0.2	1.77E+12	1.77E+12	9.90E+01	5.61E-11
32	10	2.63E+67	2.63E+67	1.31E+58	4.97E-10	0.2	1.13E+13	1.13E+13	6.26E+03	5.54E-10
33	10	8.68E+69	8.68E+69	5.22E+60	6.01E-10	0.2	7.46E+13	7.46E+13	2.02E+04	2.71E-10
34	10	2.95E+72	2.95E+72	1.25E+62	4.23E-11	0.2	5.07E+14	5.07E+14	2.64E+05	5.20E-10
35	10	1.03E+75	1.03E+75	5.46E+66	5.28E-09	0.2	3.55E+15	3.55E+15	1.03E+07	2.91E-09
36	10	3.72E+77	3.72E+77	5.22E+68	1.40E-09	0.2	2.56E+16	2.56E+16	1.25E+08	4.87E-09

TABLE AV: **Errors of BB/FG's algorithm for complex matrices.** We did the precision test by computing the permanent of an $N \times N$ all-r complex matrix, in which each element has a complex value of r ("Value of Elements"). In this case, the ideal permanent is $r^N \cdot N!$ ("Theoretical Value"), where N is the size of the matrix ("Size of Matrix"). "Computing Value" is the result produced by BB/FG's algorithm, which contains two parts: the real part, denoted by "Re. Part" and the imaginary part, denoted by "Im. Part". The "Abs. Error" is calculated following $Error_{\text{Abs.}} = \sqrt{(Re_{\text{computing}} - Re_{\text{Theoretical}})^2 + (Im_{\text{computing}} - Im_{\text{Theoretical}})^2}$, and the relative error rate is $\frac{Error_{\text{Abs.}}}{|Value_{\text{Theoretical}}|}$.

Size of Matrix	Value of Elements	Computing Value Re. Part	Computing Value Im. Part	Theoretical Value Re. Part	Theoretical Value Im. Part	Abs. Error	Relative Error Rate
17	$1+i$	9.11E+16	9.11E+16	9.11E+16	9.11E+16	4.30E+02	3.34E-15
18	$1+i$	0.00E+00	3.28E+18	0.00E+00	3.28E+18	7.01E+04	2.14E-14
19	$1+i$	-6.23E+19	6.23E+19	-6.23E+19	6.23E+19	1.14E+06	1.29E-14
20	$1+i$	-2.49E+21	0.00E+00	-2.49E+21	0.00E+00	1.99E+07	8.00E-15
21	$1+i$	-5.23E+22	-5.23E+22	-5.23E+22	-5.23E+22	4.10E+09	5.55E-14
22	$1+i$	-1.57E+10	-2.30E+24	0.00E+00	-2.30E+24	2.11E+11	9.14E-14
23	$1+i$	5.29E+25	-5.29E+25	5.29E+25	-5.29E+25	3.45E+13	4.61E-13
24	$1+i$	2.54E+27	-3.49E+12	2.54E+27	0.00E+00	1.34E+15	5.27E-13
25	$1+i$	6.35E+28	6.35E+28	6.35E+28	6.35E+28	4.78E+16	5.32E-13
26	$1+i$	1.49E+17	3.30E+30	0.00E+00	3.30E+30	1.60E+19	4.84E-12
27	$1+i$	-8.92E+31	8.92E+31	-8.92E+31	8.92E+31	1.70E+21	1.35E-11
28	$1+i$	-5.00E+33	-5.16E+19	-5.00E+33	0.00E+00	8.10E+21	1.62E-12
29	$1+i$	-1.45E+35	-1.45E+35	-1.45E+35	-1.45E+35	3.37E+24	1.64E-11
30	$1+i$	-7.79E+23	-8.69E+36	0.00E+00	-8.69E+36	1.12E+27	1.29E-10
31	$1+i$	2.69E+38	-2.69E+38	2.69E+38	-2.69E+38	6.36E+28	1.67E-10
32	$1+i$	1.72E+40	0.00E+00	1.72E+40	0.00E+00	8.40E+30	4.87E-10
33	$1+i$	5.69E+41	5.69E+41	5.69E+41	5.69E+41	3.66E+32	4.55E-10
34	$1+i$	0.00E+00	3.87E+43	0.00E+00	3.87E+43	6.09E+33	1.57E-10
35	$1+i$	-1.35E+45	1.35E+45	-1.35E+45	1.35E+45	1.36E+40	7.12E-06
36	$1+i$	-9.75E+46	-1.13E+35	-9.75E+46	0.00E+00	5.58E+38	5.72E-09
17	$10+10i$	9.11E+33	9.11E+33	9.11E+33	9.11E+33	2.40E+20	1.86E-14
18	$10+10i$	0.00E+00	3.28E+36	0.00E+00	3.28E+36	6.02E+22	1.84E-14
19	$10+10i$	-6.23E+38	6.23E+38	-6.23E+38	6.23E+38	2.13E+25	2.41E-14
20	$10+10i$	-2.49E+41	-3.30E+26	-2.49E+41	0.00E+00	5.00E+27	2.01E-14
21	$10+10i$	-5.23E+43	-5.23E+43	-5.23E+43	-5.23E+43	2.69E+30	3.63E-14
22	$10+10i$	-3.05E+32	-2.30E+46	0.00E+00	-2.30E+46	1.43E+33	6.22E-14
23	$10+10i$	5.29E+48	-5.29E+48	5.29E+48	-5.29E+48	1.17E+36	1.57E-13
24	$10+10i$	2.54E+51	1.70E+38	2.54E+51	0.00E+00	2.91E+39	1.15E-12
25	$10+10i$	6.35E+53	6.35E+53	6.35E+53	6.35E+53	2.15E+42	2.40E-12
26	$10+10i$	6.58E+42	3.30E+56	0.00E+00	3.30E+56	3.67E+44	1.11E-12
27	$10+10i$	-8.92E+58	8.92E+58	-8.92E+58	8.92E+58	8.63E+47	6.84E-12
28	$10+10i$	-5.00E+61	1.32E+47	-5.00E+61	0.00E+00	6.91E+50	1.38E-11
29	$10+10i$	-1.45E+64	-1.45E+64	-1.45E+64	-1.45E+64	2.47E+54	1.21E-10
30	$10+10i$	1.37E+53	-8.69E+66	0.00E+00	-8.69E+66	5.48E+56	6.31E-11
31	$10+10i$	2.69E+69	-2.69E+69	2.69E+69	-2.69E+69	5.89E+59	1.55E-10
32	$10+10i$	1.72E+72	0.00E+00	1.72E+72	0.00E+00	8.57E+62	4.97E-10
33	$10+10i$	5.69E+74	5.69E+74	5.69E+74	5.69E+74	4.84E+65	6.01E-10
34	$10+10i$	-1.65E+65	3.87E+77	0.00E+00	3.87E+77	1.64E+67	4.23E-11
35	$10+10i$	-1.35E+80	1.35E+80	-1.35E+80	1.35E+80	1.36E+75	7.11E-06
36	$10+10i$	-9.75E+82	-2.95E+69	-9.75E+82	0.00E+00	1.37E+74	1.40E-09

TABLE AVI: **Errors of Ryser's algorithm for real matrices.** Some data in FIG. 4 come from this table. We did the precision test by computing the permanent of an $N \times N$ all-r real matrix, in which each element has a real value of r ("Value of Elements"). In this case, the ideal permanent is $r^N \cdot N!$ ("Theor. Value"), where N is the size of the matrix ("Size of Matrix"). "Comput. Value" is the result produced by Ryser's algorithm. The "Abs. Error" is the absolute difference between the computing value and the theoretical value, and "Relative Error Rate" is the relative error rate.

Size of Matrix	Value of Elements	Comput. Value	Theor. Value	Abs. Error	Relative Error Rate	Value of Elements	Comput. Value	Theor. Value	Abs. Error	Relative Error Rate
17	1	3.56E+14	3.56E+14	3.08E+06	8.67E-09	0.1	4.03E-04	4.03E-04	2.00E-07	4.96E-04
18	1	6.40E+15	6.40E+15	7.86E+07	1.23E-08	0.1	3.63E-04	3.63E-04	1.20E-07	3.31E-04
19	1	1.22E+17	1.22E+17	8.14E+09	6.69E-08	0.1	3.63E-04	3.63E-04	1.20E-07	3.31E-04
20	1	2.43E+18	2.43E+18	3.80E+11	1.56E-07	0.1	3.99E-04	3.99E-04	1.68E-07	4.21E-04
21	1	5.11E+19	5.11E+19	2.94E+13	5.75E-07	0.1	4.79E-04	4.79E-04	1.60E-09	3.34E-06
22	1	1.12E+21	1.12E+21	2.08E+15	1.85E-06	0.1	6.23E-04	6.23E-04	2.98E-07	4.78E-04
23	1	2.59E+22	2.59E+22	5.99E+16	2.32E-06	0.1	8.72E-04	8.72E-04	2.17E-07	2.49E-04
24	1	6.20E+23	6.20E+23	1.15E+18	1.85E-06	0.1	1.31E-03	1.31E-03	3.26E-07	2.49E-04
25	1	1.55E+25	1.55E+25	2.27E+21	1.47E-04	0.1	2.09E-03	2.09E-03	2.79E-07	1.33E-04
26	1	4.03E+26	4.03E+26	4.62E+22	1.15E-04	0.1	3.56E-03	3.56E-03	1.26E-07	3.53E-05
27	1	1.09E+28	1.09E+28	2.51E+24	2.30E-04	0.1	6.40E-03	6.40E-03	3.74E-07	5.84E-05
28	1	3.05E+29	3.05E+29	3.26E+25	1.07E-04	0.1	1.22E-02	1.22E-02	4.90E-07	4.03E-05
29	1	8.67E+30	8.84E+30	1.73E+29	1.95E-02	0.1	2.43E-02	2.43E-02	2.01E-08	8.25E-07
30	1	2.85E+32	2.65E+32	1.94E+31	7.32E-02	0.1	5.11E-02	5.11E-02	5.78E-08	1.13E-06
31	1	7.58E+33	8.22E+33	6.39E+32	7.78E-02	0.1	1.12E-01	1.12E-01	1.93E-06	1.71E-05
32	1	-2.49E+33	2.63E+35	2.66E+35	1.01E+00	0.1	2.59E-01	2.59E-01	1.22E-05	4.71E-05
33	1	8.35E+36	8.68E+36	3.31E+35	3.82E-02	0.1	6.20E-01	6.20E-01	4.60E-06	7.41E-06
34	1	3.60E+38	2.95E+38	6.44E+37	2.18E-01	0.1	1.55E+00	1.55E+00	7.27E-04	4.69E-04
35	1	-5.42E+41	1.03E+40	5.52E+41	5.34E+01	0.1	4.03E+00	4.03E+00	5.97E-03	1.48E-03
36	1	4.24E+43	3.72E+41	4.21E+43	1.13E+02	0.1	1.11E+01	1.09E+01	1.75E-01	1.60E-02
17	10	3.56E+31	3.56E+31	8.65E+22	2.43E-09	0.2	4.66E+02	4.66E+02	2.75E-06	5.91E-09
18	10	6.40E+33	6.40E+33	1.95E+25	3.04E-09	0.2	1.68E+03	1.68E+03	1.29E-06	7.66E-10
19	10	1.22E+36	1.22E+36	4.69E+28	3.85E-08	0.2	6.38E+03	6.38E+03	2.64E-04	4.13E-08
20	10	2.43E+38	2.43E+38	7.63E+31	3.14E-07	0.2	2.55E+04	2.55E+04	8.12E-03	3.18E-07
21	10	5.11E+40	5.11E+40	3.07E+34	6.02E-07	0.2	1.07E+05	1.07E+05	4.65E-01	4.34E-06
22	10	1.12E+43	1.12E+43	2.19E+36	1.95E-07	0.2	4.71E+05	4.71E+05	8.81E+00	1.87E-05
23	10	2.59E+45	2.59E+45	2.73E+40	1.06E-05	0.2	2.17E+06	2.17E+06	1.06E+02	4.90E-05
24	10	6.20E+47	6.20E+47	3.83E+43	6.17E-05	0.2	1.04E+07	1.04E+07	8.29E+01	7.96E-06
25	10	1.55E+50	1.55E+50	8.36E+46	5.39E-04	0.2	5.21E+07	5.20E+07	2.44E+04	4.69E-04
26	10	4.03E+52	4.03E+52	6.24E+49	1.55E-03	0.2	2.70E+08	2.71E+08	4.00E+05	1.48E-03
27	10	1.10E+55	1.09E+55	8.37E+52	7.68E-03	0.2	1.48E+09	1.46E+09	2.34E+07	1.60E-02
28	10	2.95E+57	3.05E+57	9.56E+55	3.13E-02	0.2	7.88E+09	8.18E+09	3.07E+08	3.75E-02
29	10	9.49E+59	8.84E+59	6.46E+58	7.31E-02	0.2	4.06E+10	4.75E+10	6.84E+09	1.44E-01
30	10	1.92E+62	2.65E+62	7.31E+61	2.75E-01	0.2	6.61E+11	2.85E+11	3.76E+11	1.32E+00
31	10	1.07E+65	8.22E+64	2.50E+64	3.04E-01	0.2	-9.00E+12	1.77E+12	1.08E+13	6.09E+00
32	10	6.54E+66	2.63E+67	1.98E+67	7.51E-01	0.2	2.86E+14	1.13E+13	2.74E+14	2.43E+01
33	10	3.60E+70	8.68E+69	2.73E+70	3.14E+00	0.2	-3.58E+15	7.46E+13	3.65E+15	4.89E+01
34	10	-8.76E+73	2.95E+72	9.06E+73	3.07E+01	0.2	3.77E+16	5.07E+14	3.72E+16	7.34E+01
35	10	1.32E+77	1.03E+75	1.31E+77	1.27E+02	0.2	-2.18E+17	3.55E+15	2.22E+17	6.25E+01
36	10	-2.14E+80	3.72E+77	2.14E+80	5.75E+02	0.2	-2.10E+19	2.56E+16	2.10E+19	8.22E+02

TABLE AVII: **Errors of Ryser's algorithm for complex matrices.** We did the precision test by computing the permanent of an $N \times N$ all-r complex matrix, in which each element has a complex value of r ("Value of Elements"). In this case, the ideal permanent is $r^N \cdot N!$ ("Theoretical Value"), where N is the size of the matrix ("Size of Matrix"). "Computing Value" is the result produced by Ryser's algorithm, which contains two parts: the real part, denoted by "Re. Part" and the imaginary part, denoted by "Im. Part". The "Abs. Error" is calculated following $Error_{\text{Abs.}} = \sqrt{(Re_{\text{computing}} - Re_{\text{Theoretical}})^2 + (Im_{\text{computing}} - Im_{\text{Theoretical}})^2}$, and the relative error rate is $\frac{Error_{\text{Abs.}}}{|Value_{\text{Theoretical}}|}$.

Size of Matrix	Value of Elements	Computing Value Re. Part	Computing Value Im. Part	Theoretical Value Re. Part	Theoretical Value Im. Part	Abs. Error	Relative Error Rate
17	$1+i$	9.11E+16	9.11E+16	9.11E+16	9.11E+16	1.12E+09	8.67E-09
18	$1+i$	0.00E+00	3.28E+18	0.00E+00	3.28E+18	4.03E+10	1.23E-08
19	$1+i$	-6.23E+19	6.23E+19	-6.23E+19	6.23E+19	5.89E+12	6.69E-08
20	$1+i$	-2.49E+21	0.00E+00	-2.49E+21	0.00E+00	3.89E+14	1.56E-07
21	$1+i$	-5.23E+22	-5.23E+22	-5.23E+22	-5.23E+22	4.25E+16	5.75E-07
22	$1+i$	-5.91E+17	-2.30E+24	0.00E+00	-2.30E+24	4.31E+18	1.87E-06
23	$1+i$	5.29E+25	-5.29E+25	5.29E+25	-5.29E+25	1.73E+20	2.32E-06
24	$1+i$	2.54E+27	-6.38E+21	2.54E+27	0.00E+00	7.92E+21	3.12E-06
25	$1+i$	6.35E+28	6.35E+28	6.35E+28	6.35E+28	1.33E+25	1.48E-04
26	$1+i$	1.44E+24	3.30E+30	0.00E+00	3.30E+30	6.83E+26	2.07E-04
27	$1+i$	-8.92E+31	8.92E+31	-8.92E+31	8.92E+31	2.90E+28	2.30E-04
28	$1+i$	-5.00E+33	2.40E+29	-5.00E+33	0.00E+00	5.85E+29	1.17E-04
29	$1+i$	-1.42E+35	-1.42E+35	-1.45E+35	-1.45E+35	4.00E+33	1.95E-02
30	$1+i$	3.91E+34	-9.33E+36	0.00E+00	-8.69E+36	6.37E+35	7.33E-02
31	$1+i$	2.48E+38	-2.48E+38	2.69E+38	-2.69E+38	2.96E+37	7.78E-02
32	$1+i$	-1.63E+38	0.00E+00	1.72E+40	0.00E+00	1.74E+40	1.01E+00
33	$1+i$	5.47E+41	5.47E+41	5.69E+41	5.69E+41	3.07E+40	3.82E-02
34	$1+i$	0.00E+00	4.71E+43	0.00E+00	3.87E+43	8.45E+42	2.18E-01
35	$1+i$	7.10E+46	-7.10E+46	-1.35E+45	1.35E+45	1.02E+47	5.34E+01
36	$1+i$	-1.11E+49	7.42E+47	-9.75E+46	0.00E+00	1.10E+49	1.13E+02
17	$10+10i$	9.11E+33	9.11E+33	9.11E+33	9.11E+33	3.13E+25	2.43E-09
18	$10+10i$	0.00E+00	3.28E+36	0.00E+00	3.28E+36	9.97E+27	3.04E-09
19	$10+10i$	-6.23E+38	6.23E+38	-6.23E+38	6.23E+38	3.39E+31	3.85E-08
20	$10+10i$	-2.49E+41	7.02E+33	-2.49E+41	0.00E+00	7.84E+34	3.15E-07
21	$10+10i$	-5.23E+43	-5.23E+43	-5.23E+43	-5.23E+43	3.98E+37	5.38E-07
22	$10+10i$	-2.36E+40	-2.30E+46	0.00E+00	-2.30E+46	2.72E+40	1.18E-06
23	$10+10i$	5.29E+48	-5.29E+48	5.29E+48	-5.29E+48	6.10E+43	8.15E-06
24	$10+10i$	2.54E+51	-4.61E+46	2.54E+51	0.00E+00	1.15E+47	4.54E-05
25	$10+10i$	6.36E+53	6.36E+53	6.35E+53	6.35E+53	4.44E+50	4.94E-04
26	$10+10i$	1.25E+52	3.30E+56	0.00E+00	3.30E+56	5.12E+53	1.55E-03
27	$10+10i$	-8.99E+58	8.99E+58	-8.92E+58	8.92E+58	9.69E+56	7.68E-03
28	$10+10i$	-4.84E+61	4.78E+58	-5.00E+61	0.00E+00	1.57E+60	3.14E-02
29	$10+10i$	-1.55E+64	-1.55E+64	-1.45E+64	-1.45E+64	1.50E+63	7.31E-02
30	$10+10i$	3.25E+64	-6.30E+66	0.00E+00	-8.69E+66	2.39E+66	2.76E-01
31	$10+10i$	3.51E+69	-3.51E+69	2.69E+69	-2.69E+69	1.16E+69	3.04E-01
32	$10+10i$	4.29E+71	0.00E+00	1.72E+72	0.00E+00	1.30E+72	7.51E-01
33	$10+10i$	2.36E+75	2.36E+75	5.69E+74	5.69E+74	2.53E+75	3.14E+00
34	$10+10i$	-5.63E+77	1.15E+79	0.00E+00	3.87E+77	1.11E+79	2.87E+01
35	$10+10i$	-1.73E+82	1.73E+82	-1.35E+80	1.35E+80	2.43E+82	1.27E+02
36	$10+10i$	5.60E+85	1.69E+82	-9.75E+82	0.00E+00	5.61E+85	5.75E+02

TABLE AVIII: **Errors of Ryser's algorithm from the order of addition operations.** "Size of Matrix" is the problem scale tested. "Theor. Value" is the theoretical value, "Original Order" is the basic order of Ryser's algorithm in Algorithm 1, "Random Order" is to do the summation randomly, "Merge" indicates the summation is done 2 numbers by 2 numbers; "Separate Addition" denotes that the result is obtained through a substraction between the all the added numbers (corresponding to the even $|S|$) and the subtracted numbers, which may produces the worst error.

Scale of	Theor.	Original Order		Random Order		Merge		Separate Addition	
Matrix	Value	Value	Error Rate	Value	Error Rate	Value	Error Rate	Value	Error Rate
8	4.03E+04	4.03E+04	0.00E+00	4.03E+04	0.00E+00	4.03E+04	0.00E+00	4.03E+04	0.00E+00
9	3.63E+05	3.63E+05	0.00E+00	3.63E+05	0.00E+00	3.63E+05	0.00E+00	3.63E+05	0.00E+00
10	3.63E+06	3.63E+06	0.00E+00	3.63E+06	0.00E+00	3.63E+06	0.00E+00	3.63E+06	0.00E+00
11	3.99E+07	3.99E+07	0.00E+00	3.99E+07	0.00E+00	3.99E+07	0.00E+00	3.99E+07	0.00E+00
12	4.79E+08	4.79E+08	0.00E+00	4.79E+08	0.00E+00	4.79E+08	0.00E+00	4.79E+08	0.00E+00
13	6.23E+09	6.23E+09	0.00E+00	6.23E+09	0.00E+00	6.23E+09	0.00E+00	6.23E+09	0.00E+00
14	8.72E+10	8.72E+10	0.00E+00	8.72E+10	1.32E-07	8.72E+10	0.00E+00	8.72E+10	9.18E-09
15	1.31E+12	1.31E+12	1.96E-10	1.31E+12	3.62E-07	1.31E+12	4.86E-10	1.31E+12	2.35E-08
16	2.09E+13	2.09E+13	8.81E-10	2.09E+13	1.29E-07	2.09E+13	9.57E-10	2.09E+13	1.36E-07
17	3.56E+14	3.56E+14	1.11E-08	3.56E+14	9.41E-05	3.56E+14	8.24E-09	3.56E+14	4.81E-07
18	6.40E+15	6.40E+15	7.73E-09	6.40E+15	1.46E-04	6.40E+15	2.59E-09	6.40E+15	2.57E-06
19	1.22E+17	1.22E+17	4.28E-08	1.22E+17	1.72E-04	1.22E+17	8.13E-08	1.22E+17	7.31E-05
20	2.43E+18	2.43E+18	2.60E-07	2.39E+18	1.64E-02	2.43E+18	2.46E-07	2.43E+18	4.51E-04
21	5.11E+19	5.11E+19	9.52E-07	3.64E+19	2.88E-01	5.11E+19	1.01E-06	5.11E+19	9.39E-04
22	1.12E+21	1.12E+21	2.88E-06	-3.60E+20	1.32E+00	1.12E+21	4.28E-06	1.14E+21	1.59E-02
23	2.59E+22	2.59E+22	4.15E-06	6.96E+23	2.59E+01	2.59E+22	1.39E-05	2.72E+22	5.02E-02
24	6.20E+23	6.20E+23	1.59E-05	-1.21E+25	2.04E+01	6.20E+23	2.18E-05	7.80E+23	2.57E-01
25	1.55E+25	1.55E+25	1.05E-04	-5.49E+27	3.55E+02	1.55E+25	1.28E-04	-3.50E+25	3.26E+00
26	4.03E+26	4.03E+26	1.53E-04	2.29E+30	5.67E+03	4.03E+26	4.36E-04	1.68E+28	4.07E+01
27	1.09E+28	1.09E+28	5.48E-04	-1.36E+32	1.25E+04	1.09E+28	1.35E-03	-2.95E+30	2.72E+02
28	3.05E+29	3.05E+29	1.83E-04	1.61E+34	5.27E+04	3.05E+29	1.12E-04	4.66E+32	1.53E+03
29	8.84E+30	8.54E+30	3.47E-02	-6.42E+36	7.26E+05	8.47E+30	4.16E-02	-1.08E+35	1.22E+04
30	2.65E+32	2.97E+32	1.18E-01	-7.86E+38	2.96E+06	2.98E+32	1.23E-01	3.13E+37	1.18E+05
31	8.22E+33	6.15E+33	2.53E-01	7.00E+41	8.52E+07	5.81E+33	2.94E-01	1.75E+38	2.12E+04
32	2.63E+35	8.21E+34	6.88E-01	-8.38E+43	3.19E+08	1.24E+35	5.29E-01	2.65E+41	1.01E+06

TABLE AIX: **Results comparing BB/FG's algorithm and Ryser's algorithm for random unitary matrices.** Some data of "Random unitary matrix" in FIG. 5 come from this table. "Size of Matrix" is the problem scale tested. "Results of Ryser" indicates the computing value from Ryser's algorithm, represented in real part and imaginary part. "Results of BB/FG" indicates the computing value from BB/FG's algorithm. The Relative Error Rate in Modulus is calculated by $\frac{|Perm_{\mathrm{BB/FG}}-Perm_{\mathrm{Ryser}}|}{|Perm_{\mathrm{BB/FG}}|}$. The matrices used as the testing cases are generated by MATLAB.

Size of	Results of Ryser		Results of BB/FG		Relative Error
Matrix	Re. Part	Im. Part	Re Part	Im. Part	Rate in Modulus
31	4.2230E-09	-1.9454E-09	4.2230E-09	-1.9454E-09	0
32	-4.1659E-09	-2.3246E-09	-4.1659E-09	-2.3246E-09	0
33	4.8134E-10	8.4106E-10	4.8134E-10	8.4106E-10	0
34	2.7587E-10	2.1718E-10	2.7587E-10	2.1718E-10	2.848E-07
35	-1.1053E-10	-7.2113E-10	-1.1053E-10	-7.2113E-10	1.371E-07
36	-5.5166E-11	-3.4459E-11	-5.5166E-11	-3.4459E-11	4.612E-07
37	-3.3585E-11	3.9724E-12	-3.3585E-11	3.9722E-12	5.039E-06
38	-5.6397E-11	-6.3709E-11	-5.6397E-11	-6.3709E-11	2.351E-07
39	-4.2777E-11	-1.2135E-11	-4.2777E-11	-1.2135E-11	4.498E-07
40	5.8951E-12	-2.1875E-11	5.8951E-12	-2.1875E-11	0

TABLE AX: **Results comparing BB/FG's algorithm and Ryser's algorithm for random-derived matrices.** Some data of "Random-derived matrix" in FIG. 5 come from this table. "Size of Matrix" is the problem scale tested. "Results of Ryser" indicates the computing value from Ryser's algorithm, represented in real part and imaginary part. "Results of BB/FG" indicates the computing value from BB/FG's algorithm. The Relative Error Rate in Modulus is calculated by $\frac{|Perm_{\mathrm{BB/FG}}-Perm_{\mathrm{Ryser}}|}{|Perm_{\mathrm{BB/FG}}|}$. The matrices used were derived from a 100×100 unitary matrix.

Size of	Results of Ryser		Results of BB/FG		Relative Error
Matrix	Re. Part	Im. Part	Re. Part	Im. Part	Rate in Modulus
21	-4.3428E-12	-5.9702E-12	-4.3428E-12	-5.9702E-12	0
22	7.6833E-13	-3.9798E-13	7.6833E-13	-3.9798E-13	1.1557E-07
23	-3.7027E-12	1.6829E-12	-3.7027E-12	1.6829E-12	0
24	-3.4145E-12	1.6790E-12	-3.4145E-12	1.6790E-12	0
25	6.3631E-13	6.0936E-13	6.3631E-13	6.0936E-13	0
26	2.0950E-13	-3.6558E-13	2.0950E-13	-3.6558E-13	0
27	1.7856E-13	1.7049E-13	1.7856E-13	1.7049E-13	0
28	-1.4828E-14	-5.6576E-14	-1.4828E-14	-5.6576E-14	0
29	9.6421E-14	2.0312E-13	9.6421E-14	2.0312E-13	0
30	1.7654E-14	2.7364E-14	1.7654E-14	2.7364E-14	0
31	2.7628E-16	1.4029E-14	2.7628E-16	1.4029E-14	7.1269E-09
32	-1.7119E-14	1.3498E-14	-1.7119E-14	1.3498E-14	0
33	6.9880E-15	4.0715E-15	6.9880E-15	4.0715E-15	0
34	1.0924E-15	1.2235E-14	1.0924E-15	1.2235E-14	0
35	-1.0497E-16	-1.3781E-16	-1.0497E-16	-1.3781E-16	0
36	5.9267E-16	-1.9652E-16	5.9268E-16	-1.9652E-16	3.2030E-06
37	-3.5034E-16	-2.3051E-16	-3.5034E-16	-2.3051E-16	0
38	2.7198E-15	6.0656E-16	2.7198E-15	6.0656E-16	0
39	7.9334E-16	5.6975E-16	7.9334E-16	5.6975E-16	2.4763E-06
40	1.2277E-16	-2.4051E-16	1.2276E-16	-2.4051E-16	2.0768E-05
41	-1.2519E-16	1.7989E-16	-1.2519E-16	1.7989E-16	1.2905E-06
42	-5.1615E-16	-3.3737E-16	-5.1618E-16	-3.3742E-16	9.6984E-05
43	-8.8131E-17	3.3867E-16	-9.0932E-17	3.3741E-16	8.7707E-03
44	1.3425E-18	1.0379E-19	1.3424E-18	1.0375E-19	5.9686E-05

TABLE AXI: **Results comparing BB/FG's algorithm and Ryser's algorithm for special-derived matrices.** Some data of "Special-derived matrix" in FIG. 5 come from this table. "Size of Matrix" is the problem scale tested. "Results of Ryser" indicates the computing value from Ryser's algorithm. "Results of BB/FG" indicates the computing value from BB/FG's algorithm. The Relative Error Rate in Modulus is calculated by $\frac{|Perm_{\mathrm{BB/FG}}-Perm_{\mathrm{Ryser}}|}{|Perm_{\mathrm{BB/FG}}|}$. The matrices used were manually chosen from the 100×100 real unitary matrix with elements all negative, and duplicated the rows and columns to enlarge the scale.

Size of	Results of	Results of	Relative Error
Matrix	Ryser's algorithm	BB/FG's algorithm	Rate in Modulus
30	5.3072E-01	4.6606E-01	1.3874E-01
31	-2.2483E-01	-1.2863E-01	7.4793E-01
32	1.1668E+00	7.4303E-01	5.7034E-01
33	6.3670E+01	-3.6957E+00	1.8228E+01
34	3.5526E+01	2.1389E-01	1.6510E+02
35	1.4313E+04	-7.9309E+02	1.9047E+01
36	2.8634E+04	3.1883E+02	8.8812E+01
37	6.3388E+04	-7.0710E+01	8.9745E+02
38	1.3012E+07	2.5863E+03	5.0300E+03
39	-1.0717E+07	-4.8804E+03	2.1950E+03
40	-1.0307E+08	1.2365E+03	8.3360E+04

TABLE AXII: **Fitting Result** This table shows the fitting result of curve in FIG. 3.

Result:			
Cofficients	**Value**	**95% confidence bounds**	
		lower bound	**upper bound**
a:	9.805×10^{-12}	9.245×10^{-12}	1.037×10^{-11}
b:	-0.87782	-0.8916	-0.8649
Goodness of fitting:			
SSE:	284.2	The small, the better	
R_square:	0.994	The more close to 1, the better	
Adjusted R_square:	0.9938		
RMSE:	2.665	The small, the better	